THE JOURNAL OF PHYSICAL CHEMISTRY B

Article

pubs.acs.org/JPCB

Dynamic Deuterium Magic Angle Spinning NMR of a Molecule Grafted at the Inner Surface of a Mesoporous Material

S. Jayanthi,[†] V. Frydman,[†] and S. Vega*,[†]

[†]Department of Chemical Physics, Weizmann Institute of Science, Rechovot, Israel 76100

Supporting Information

ABSTRACT: Deuterium magic angle spinning (MAS) NMR is used to study the dynamics of an organic molecule, *N*-[triethoxysilylpropyl]acetamide-d_3, grafted at the inner surface of the mesoporous silica material, MCM-41. The grafted molecule has a deuterated methyl group at its free terminus to monitor its local mobility through changes in its dynamic ^{2}H-MAS NMR spectrum. Different spectra were recorded as a function of temperature from two different water containing samples. Observation shows that a major part of the grafted molecule remains static, irrespective of the temperature and hydration state of the sample, whereas the rest shows spectral changes indicative of a two-site jump motion of the methyl groups. Experimental observations were substantiated using molecular dynamic (MD) simulations of the grafted molecule. Subsequently, the MD results corroborate a model for the grafted molecules experiencing an exchange between two conformations consistent with the analysis of the ^{2}H-MAS NMR spectra.

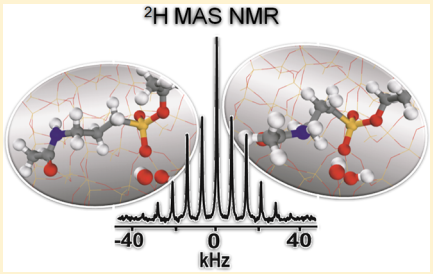

INTRODUCTION

Dynamics of molecules located at organic and inorganic surfaces have always been an area of interest due to their extended applicability in various fields. Beginning with their discovery in the early 1990s, ordered mesoporous silicas showing large surface areas have attracted considerable interest as catalysts, adsorbents, and substrates for optical, electronic, and magnetic materials. Due to their large void pore volume (with radii 1−10 nm), they allow diffusion of molecules through the pores that further leads to their adsorption on a variety of surface binding sites. Over the past decade silica based organic−inorganic hybrid materials have been investigated for catalytic reactions. Identifying the structure−function relationship of these silica-supported organic−inorganic hybrid materials enhances the knowledge of these systems together with the possibility of using them for catalysis, storage, etc.[1−4] Several studies have been reported on the adsorption and mobility of adsorbates close to these surfaces, using various techniques including solid state NMR.[5−19] The functionality of these materials has been modified by various kinds of covalently attached (grafted) polymers at their inner surface. A number of characterization techniques have been given in the literature to characterize molecular layers on surfaces that can collectively provide structural information at a molecular and an atomic level.[5−13]

Dynamic studies of adsorbed molecules in mesoporous silica materials have been reported earlier by employing ^{2}H MAS NMR and analyzing the changes in the sideband spectra due to motional averaging effects.[12−14] In the present study, we attempt to look at the dynamics of a small organic molecule (*N*-[triethoxysilylpropyl]acetamide-d_3) grafted at the inner surface of a mesoporous material, MCM41. Restricted motion of the molecules is characterized using ^{2}H-MAS NMR of the terminal CD_3 group. Surface characterization studies of similar systems have been reported using solid state MAS NMR by monitoring ^{1}H and ^{13}C relaxation rates and by analyzing ^{2}H MAS spectra.[5,20,21] One of the major challenges for solid state NMR in studying these systems is the lack of sensitivity because of the low concentration of the molecules grafted to the surface (usually ∼1 molecule/nm^2). Low concentrations are a necessary condition to avoid largely the possibility of intermolecular interactions. ^{2}H MAS NMR becomes highly relevant in this context.

Deuterium NMR stands out as a powerful probe for dynamic studies of molecules because of numerous merits. These include the dependence of line positions on the orientation of the $I = 1$ quadrupole tensor fixed to bond axes, and the slow spin diffusion between deuterons and hence the presence of purely motional induced relaxation times highly sensitive to dynamics from time scales ranging from 10 to 10^{12} s^{-1}. Perhaps most important are the numerous analytical and numerical tools available for the analysis of dynamic ^{2}H spectra. Accurate analysis of static and MAS spectra of deuterium has been possible because of its small quadrupolar coupling constants (50−200 kHz), which enables excitation of whole spectra using single high power RF pulses.

The dynamics of molecules have been reported in the literature time and again using solid state NMR by exploiting the orientational dependence of deuterium nuclei. Spiess and co-workers performed several complete studies on the molecular mobility of linear polymers using deuterium static solid state NMR of deuterated methyl or methylene

Received: June 21, 2012
Revised: August 1, 2012
Published: August 1, 2012

dx.doi.org/10.1021/jp3061152 | J. Phys. Chem. B 2012, 116, 10398−10405

groups.[22−26] Subsequently, monitoring segmental motion on various linear polymers or segmented copolymers through deuterium static solid state NMR has been reported by many in various contexts.[27−32] Well-employed intramolecular motional model reported in the literature in many linear chain systems resembles a trans−gauche isomerization.[30−34] The majority of the spectral analysis was based on the general formalism proposed by Torchia and Szabo.[35] In general, the above studies point to the fact that, for linear chain molecules, trans−gauche isomerization is one of the most probable conformational changes. In the present study deuterium MAS NMR is used to probe the restricted dynamics of a similar chain grafted at the inner surface of MCM-41.

Characterization of mesoporous materials has been addressed by many groups in various contexts. The mobility of grafted molecules is closely associated with the characteristics of the system to which it is grafted. Silica surfaces in MCM-41 type of materials are composed of siloxanes ($(OH)SiO_3$) and silanols ($(OH)_2SiO_2$), which occupy a significant fraction of the surface silica and may exist as isolated, geminal, or vicinal −OH groups.[36,37] These groups play an important role in the function and properties of the surface and hence affect the local mobility of the adsorbed or grafted molecules.

As stated above, the free terminus of the grafted molecule in this study has a methyl group that is deuterated to monitor the dynamics of the orientation of its ^{2}H quadrupolar tensors due to changes in temperature and hydration levels of the surface. ^{2}H MAS spectra were recorded for two levels of hydration within the temperature range 200−315 K. Spectral analysis along with supporting molecular dynamics (MD) simulations are presented providing the local mobility of the grafted molecules in the pores. Toward the end, the role of single water molecules inducing mobility is briefly discussed.

MATERIALS AND METHODS

Grafting Procedure. MCM-41 was purchased from Sigma Aldrich and used without further purification. The surface area of MCM-41 is 1000 m^2/g and its pore diameter ∼3 nm. The synthesis and the grafting protocol of *N*-[(3-triethoxysilyl)-propyl] acetamide-d_3 (**1**) are as given below.

Step 1. Acetic acid-d_4 (0.5 mL, 8.7 mmol) and *N*-hydroxysuccinimide (NHS) (1.105 g, 9.6 mmol) were dissolved in dry tetrahydrofuran (30 mL) (THF). The solution was treated with dicyclohexylcarbodimide (1.98 g, 9.6 mmol) (DCC) and stirred under nitrogen in an ice−water bath for 1 h. The cooling bath was then removed, and the mixture was flushed with nitrogen, sealed, and stirred at room temperature overnight. The precipitated urea was filtered off, and the filtrate was evaporated, affording the NHS activated ester as a white solid, which was used in the next step without further purification.

Step 2. The activated ester prepared above (0.378 g, 2.36 mmol) and (3-aminopropyl)triethoxysilane (0.538 g, 2.43 mmol) were dissolved in dry dichloromethane (15 mL) under nitrogen. To this solution, triethylamine (0.248 g, 2.45 mmol) was added, and the mixture was flushed with nitrogen, sealed, and stirred at room temperature overnight. The solvent was evaporated, and the residue was stirred with a mixture of dry hexane (20 mL) and dry ethyl acetate (3 mL). The precipitated white solid (NHS) was filtered off, and the filtrate was evaporated, affording **1** as a thick oil. ESIMS (ES^+): *m*/*z* 289.12 ($[M + Na]^+$, 100), 305.10 ($[M + K]^+$, 12), 555.31 ($[2M + Na]^+$, 8).

Step 3. For grafting of compound **1** on MCM-41, MCM-41 (0.2 g) (previously dried at 297 K for 4 h) was mixed with the deuterated compound **1** (0.126 g, 0.472 mmol) and dry toluene (3 mL) was added. The mixture was heated at reflux under nitrogen for 4 h. The suspension was allowed to cool to room temperature, and the mesoporous material was collected by filtration, washed thoroughly with dry toluene, and dried under vacuum.

The overall synthesis can be represented as

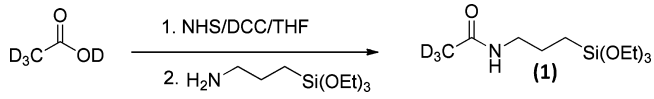

Solid State NMR. All experiments were done on Bruker DSX 300 MHz equipped with 4 mm triple resonance MAS probe. Approximately 40 mg of sample was packed in a 4 mm rotor. Subsequently, it was kept in a closed environment with 3 μL of double distilled water overnight for wetting and the increase in the sample weight was monitored. ^{1}H and ^{2}H 1D MAS spectra were recorded at a 6 kHz spinning rate using a single 90° excitation pulse. The pulse lengths used were 5 and 2.5 μs for deuterium and proton with a recycle delay of 0.3 and 1 s, respectively. MAS experiments were recorded at various temperatures ranging from 200 to 315 K. ^{29}Si CPMAS[38] was recorded at 10 kHz MAS with a Bruker AV-III 500 MHz spectrometer

Simulations. Deuterium powder simulations were done for various quadrupole tensor parameters using the SIMPSON simulation package with 1154 crystal orientations.[39] All other simulations were done using home build MATLAB programs. Molecular dynamics (MD) simulations were done using the Accelerys Material Studio Package.[40]

Basic Setup of MD and the COMPASS Force Field. MD simulations were performed using the Accelerys Materials Studio (MS) - v5.5 in CPU: Xeon E5620 (2.4 GHz), with 4 cores and OS as Windows Server 2008 R2. Calculations were done using the DISCOVER and the FORCITE programs from Accelerys.

Setting up a system to run MD simulation requires a careful choice of various parameters. The main parameters available are the choice of a force field, the time step, and the choice of an ensemble. One can envisage the existing molecular modeling force fields for molecular systems in terms of a simple four component picture of intra- and intermolecular forces within the system. The types of forces involved are derived from deviation from the equilibrium bond lengths and bond angles, energetic function for bond rotations and interaction between nonbonded parts of the system. The potential energies that are defined in the MD calculations include all contributions from bonded and nonbonded interactions, where the nonbonded ones consist of van der Waals, hydrogen bonding, and electrostatic interactions whereas the bonded part represents the energies of deformation of bond lengths, bond angles and the torsion angles. We have used the condensed phase optimization molecular potentials for atomistic simulation studies (COMPASS)[41−43] to describe the interactions between atoms in the MCM-41 host silica and of the guest molecule. COMPASS force field based on the polymer consistent force field (PCFF) was parametrized and tested for most common organic and inorganic small molecules and polymers.[42,43] For the simulations, we use the *NVT* (constant number, volume, and temperature) ensemble with an Andersen type algorithm for the thermostat.

dx.doi.org/10.1021/jp3061152 | J. Phys. Chem. B 2012, 116, 10398−10405

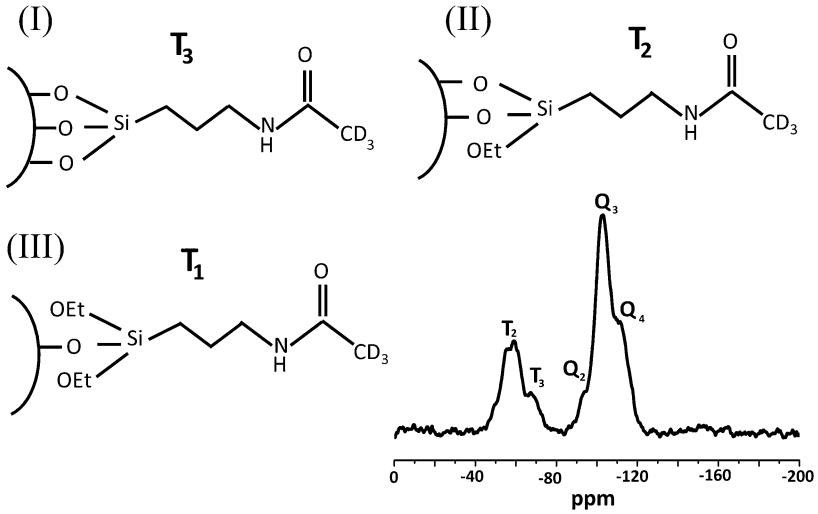

Figure 1. Schematic structure of the molecule and its possible grafting configurations in (I) T_3, (II) T_2, and (III) T_1. ^{29}Si CPMAS spectrum of post grafted MCM-41 is also shown.

Yet another crucial step is the design of the host silica surface. Mesoporous surface prior to grafting was made following the protocol described by Chaffe.[44] The initial structure was generated using the three dimensionally infinite lattice of α quartz with lattice parameters 4.91, 4.91, and 5.402 Å for *a*, *b*, and *c*, respectively. A periodic supercell of dimension 12 × 12 × 12 was created from this initial structure. A hexagonal pore of a certain diameter was created in the supercell by systematically removing the silicon and oxygen atoms from the center for a selected diameter (~3.2 nm in our case). This results in vacant bonding configurations for silicon and oxygen atoms in the pore. We have saturated the vacant silicon atoms with hydroxyl (OH) groups and the vacant oxygen atoms with hydrogen atoms. After this surface saturation procedure, the template was subjected to DISCOVER minimization followed by MD calculations for 100−200 ps. After each MD calculation, water molecules were removed from the surface, where adjacent OH groups were close enough to form OH---H hydrogen bonds (OH---H distance < ~2.5 Å) leaving an oxygen linkage to silicon, Si−O−Si, following Chaffe.[44] Care was taken to dehydrate the surface sparsely along the length of the pore as the probability of a sequential dehydration is rare in reality. This removes the possibility of a uniform distribution of hydroxyl groups along the channel. This process not only dehydrates the system but also creates Si−O−Si linkages in the surface. This was continued until the surface silanol concentration was reduced to ~2.2 OH/nm^2. The molecule under study was covalently attached to two adjacent Si atoms for further studies. The presence of net charge on the template and its subsequent effect on dynamic calculation has not been considered in this study.

RESULTS AND DISCUSSIONS

Analysis of the System Post Grafting. Grafting is the process by which a guest molecule is permanently attached to the substrate through a chemical reaction. In our case, molecule **1** is chemically bonded to the MCM-41 surface via oxygen atoms through steps 1−3. Because the surface of the mesoporous material is complex due to the presence of different types of silica configurations and surface hydroxyl groups, ^{29}Si CPMAS NMR was used to identify the binding properties of the grafted molecules via ^{29}Si chemical shifts. Three possible grafting configurations (I), (II), and (III) of *N*-[triethoxysilylpropyl]acetamide-d_3 are shown in Figure 1 along with the room temperature ^{29}Si CPMAS spectrum recorded at ambient temperature of the postgrafted MCM-41 sample. The spectrum shows the well-characterized Q_2, Q_3, and Q_4 lines with chemical shift values −90, −100, and −110 ppm, respectively. Peaks labeled as T_3 (−69 ppm) and T_2 (−58 ppm) arise from those silicon atoms that bind the grafted molecules to the surface. Deconvolution of the above spectra shows that two grafting conformations are present, (i) part of the grafted molecules are in a T_2 conformation (II), wherein the silicon of the molecules is covalently bonded to the surface via two oxygen atoms, and (ii) part of the grafted molecules are in the T_3 conformation (I), wherein the molecule binds to the surface via three oxygen atoms. Yet another observation which is characteristic of MCM-41 is its very low Q_2 line intensity that shows low concentration of surface silanols. It can be seen from the spectra that most molecules are bound via −O−(SiO)−O−, leaving one ethoxy (Et) group with the molecule after grafting. This configuration corresponds to the schematic molecular structure (II) shown in Figure 1. The presence of this configuration has been verified by a ^{13}C CP-MAS experiment (Supporting Information, Figure S1). Assignment of the peaks in the resulting spectrum indicates the presence of configuration (II), showing the presence of the ethoxy lines with chemical shifts and amplitudes consistent with the T_2 configuration. In the rest of the discussion we disregard the small amount of molecules in configuration (I).

The proton concentrations per nm^2 (p) of the samples have been determined by recording their proton spectra as a function of water loading. Hydration levels of the sample were varied by first keeping the sample in the rotor without a cap in a closed chamber with a few microliters of distilled water for a day or more. We assumed that in this time the adsorbed water gets homogeneously distributed in the MCM-41 pores. After a high hydration level was reached, water was removed in a stepwise fashion by pumping the sample for short time periods using a vacuum line. After each pumping period the weight of the sample was measured and a ^{1}H MAS spectrum, with 6 kHz spinning, was recorded. The total integrated line intensities of the spectra of these samples were correlated with their loss in weight. From the linear dependence of these intensities with

dx.doi.org/10.1021/jp3061152 | J. Phys. Chem. B 2012, 116, 10398−10405

weight loss (Supporting Information, Figure S2) we determined the values of p on the surface, using the prior knowledge of surface area per gram of our MCM-41 samples. Finally, two separate samples were prepared for our further systematic study: a "wet" sample with $p \sim 7$ and a "dry" sample with $p \sim 2$, thus differing by 2−3 water molecules per nm^2. The ^{1}H MAS spectra of these samples in Figure 2 show that there are well-

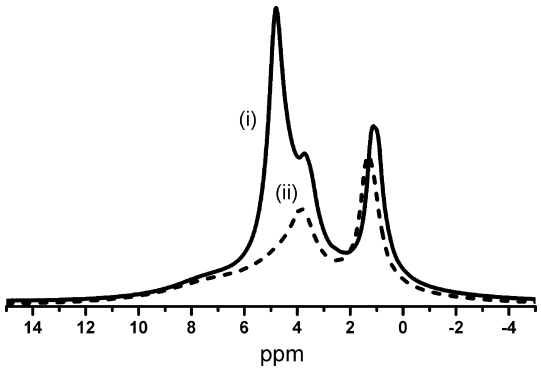

Figure 2. Proton 1D MAS spectrum recorded at 6 kHz MAS for (i) wet and (ii) dry sample.

defined spectral lines in addition to the bulk water peak at ∼5.1 ppm. Deconvolution of the spectrum of the wet sample results in the following distinct chemical shift values, 1.7 ppm corresponding to "isolated silanols", ∼4.1 ppm due to the exchange of surface water protons with the silanols, ∼1.4 ppm attributed to areas on the surface covered with monolayers of water, and ∼7.3 ppm arising from the strongly hydrogen bonded protons to the surface.[9,12] Similar decomposition of the dry sample resulted only in three well-defined spectral lines with chemical shifts equal to ∼7.3, ∼4.1, and ∼1.7 ppm.

Thus apart from the disappearance of bulk water protons in the dry state, the monolayer water areas disappear while the isolated silanols remain. The presence of the lines from the protons of the grafted molecules is not observed in these spectra, because of their broad width and low intensity. The ^{13}C CP-MAS spectra of two samples were found to be almost identical. To get dynamic information, we recorded ^{2}H MAS NMR spectra from both samples as a function of temperature.

Dynamic ^{2}H MAS NMR Spectra. ^{2}H MAS NMR on the wet and dry samples has been performed at a spinning frequency of 6 kHz in the temperature range 200−315 K. In Figure 3 MAS sideband spectra measured at 200, 260, and 315 K are shown. It can be observed that all sidebands are sharp irrespective of the state of the sample or the temperature, indicative of relatively fast dynamics of the molecule. A closer observation shows that for all the spectra, the span of the side bands remains the same but that none of these spectra resemble a single set of quadrupolar tensor parameters except the ones recorded at 200 K. Analysis of this broad component concludes that all spectra have a component that can be attributed to CD_3 moieties with fixed C_3 axes having a quadrupolar coupling constant of C_Q = 77 kHz, with η = 0 irrespective of the temperatures and hydration. At temperatures above 200 K an additional contribution with smaller quadrupolar parameters becomes more prominent and increases with an increase in temperature. Thus part of the grafted molecules contributes to the static tensor of CD_3, while the rest experiences some dynamics that results in changes in the effective quadrupolar tensor parameters $\{C_Q; \eta\}$. The difference between the spectra

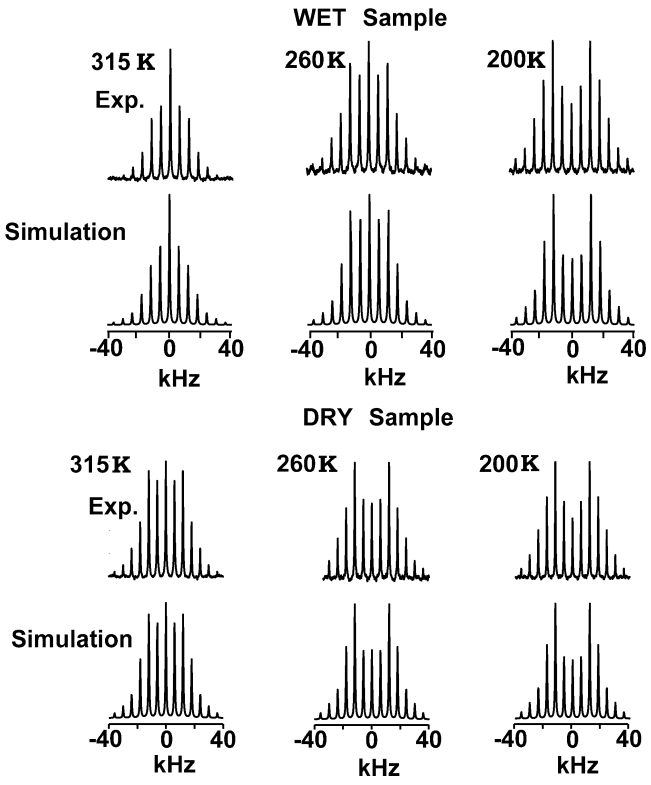

Figure 3. ^{2}H MAS spectra recorded at 6 kHz MAS rate for temperatures 315, 260, and 200 K for wet and dry samples. The corresponding simulated spectra are also shown.

of the wet and the dry samples already indicates that single water molecules can introduce enhanced mobility. From the spectra shown in Figure 3 it thus follows that an increase in the temperature and hydration level increases the dynamic component.

To further confirm these observations, nonspinning ^{2}H spectra at room temperature were recorded, using a solid echo pulse sequence. These static experiments are time-consuming because of severe reduction in sensitivity. The dominant broad part of the static spectra, as shown in Figure 4, could not be simulated with a single tensor of 77 kHz alone. A linear distribution of axially symmetric tensors ranging from 70 to 77 kHz with equal weights provided a good fit as shown in Figure

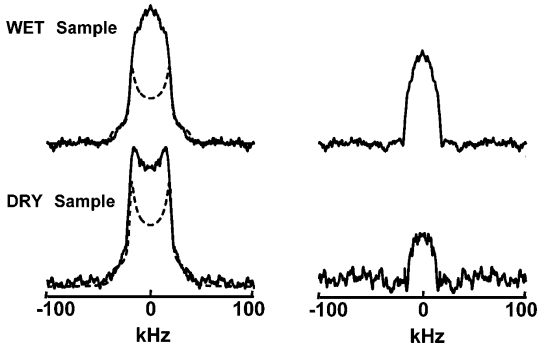

Figure 4. Static ^{2}H spectrum recorded for the wet and dry samples (solid line). The dotted line corresponds to the best fit of the static part employing a distribution of tensors ranging from 77 to 70 kHz with η = 0. The residual part obtained after subtraction of the experimental from the simulated best fit is also shown.

dx.doi.org/10.1021/jp3061152 | J. Phys. Chem. B 2012, 116, 10398−10405

4 for both wet and dry samples. The two residual parts shown in Figure 4, obtained by subtracting the fitted broad component from the experimental spectra, have the same shape and could be simulated with quadrupolar parameters $\{C_Q = 33$ kHz; $\eta = 0.7\}$. This result suggests that the motion responsible for averaging the static tensor 77−70 kHz is about the same in both wet and dry samples. To determine the relative amounts of the static and dynamic molecules as a function of hydration and temperature, the sideband spectra in Figure 3 were simulated assuming two tensor contributions. Relative intensities of the two contributions is plotted in Fgure 5,

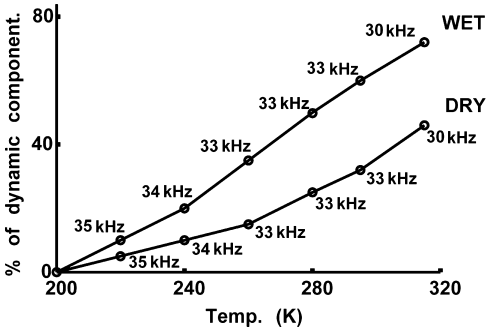

Figure 5. Graph shows the percentage of dynamic tensor as a function of temperature. The quadrupolar coupling employed for fitting the experimental spectra ($\eta = 0.7$) is shown at every temperature.

which shows that the fraction of dynamic molecules increases with temperature and that an addition of about one water molecule per nm^2 is sufficient to enhance the dynamics as well. The dynamic quadrupolar parameter C_Q and η employed for the best fit varies between 35 kHz at 220 K to 30 kHz at 315 K with $\eta \approx 0.7$. From these parameters we could conclude that we are presumably dealing with a two site jump motion of the CD_3 group, as has been observed in a large variety of molecular systems[22−32] Realizing that the chain of the grafted molecule is fixed only at one end, this conclusion must be substantiated.

From these data it is not possible to derive what are the conformational changes the grafted molecule undergoes that are responsible for averaging of the quadrupolar tensor components, from $\{C_Q = 77-70$ kHz; $\eta = 0\}$ to $\{C_Q = 35-30$ kHz; $\eta = 0\}$. To get insight into the possible conformational dynamics, MD simulations were performed to derive motional models for the terminal CD_3 group of the grafted molecules. On the basis of these models, average quadrupolar parameters can be calculated and compared with the experimental results.

Molecular Dynamic Simulations. MD simulations were performed on a grafted molecule in the binding configuration (II) as shown in Figure 2. These simulations provide the spatial time evolution of the direction of the unit vector $\bar{d}_3$ pointing along the C_3 axis of the methyl group. The deuteriums of the CD_3 groups have an averaged EFG tensor that has a set of principal values V_{PP}, $P = X, Y, Z$ and a principal axis system (PAS) frame fixed to the CD_3 group. The Z axis of the PAS frame points in the C_3 direction of the methyl group. Because the tensor is traceless and symmetric, the nuclear quadrupolar coupling constant can be expressed as $C_Q = V_{zz}eQ/h = 77$ kHz (Q is the nuclear quadrupolar moment) with $V_{XX} = V_{YY} = -V_{ZZ}/2$, which results in an axially symmetric tensor, $\eta = (V_{YY} - V_{XX})/V_{ZZ} = 0$. Due to the motion of a molecule the orientation of its CD_3 group changes causing also a change in the C_3 ($\bar{d}_3$) direction and the orientation of PAS frame of its EFG tensor.

The EFG tensor can be represented in matrix form with respect to some fixed coordinate system. This matrix has elements equal to V_{pq}, with $p, q = x, y, z$, which are a function of the principal value V_{zz} and of the orientation of the fixed frame with respect to the moving PAS frame. When the $\bar{d}_3$ unit vector, pointing in the direction of the Z-axis of the PAS frame, is defined by the (time dependent) polar angles $\{\theta, \varphi\}$ in the fixed frame, the matrix representation attains the following form.[31,32]

$$\begin{bmatrix} 3\sin^2\theta\cos^2\varphi - 1 & 3\sin^2\theta\cos\varphi\sin\varphi & 3\sin\theta\cos\theta\cos\varphi \\ 3\sin^2\theta\cos\varphi\sin\varphi & 3\sin^2\theta\sin^2\varphi - 1 & 3\sin\theta\cos\theta\sin\varphi \\ 3\sin\theta\cos\theta\cos\varphi & 3\sin\theta\cos\theta\sin\varphi & 3\cos^2\theta - 1 \end{bmatrix} \cdot V_{ZZ}$$

Simulating the $\{\theta, \varphi\}$ polar angles at equal time increments and averaging the elements of their EFG matrices followed by diagonalization, we can determine an average quadrupolar coupling constant $\bar{C}_Q$ and an average asymmetry parameter $\bar{\eta}$ corresponding to the dynamics of the CD_3 group.

For a homogeneous distribution of axial tensors with quadrupole coupling constants C_Q, with $0 < \vartheta < \Theta$ and $0 < \varphi < 2\pi$ the average tensor equals $\bar{C}_Q = C_Q \int_0^{\varphi} d\varphi \int_0^{\Theta} (3\cos^2\vartheta - 1)\sin\vartheta\, d\vartheta = 2\pi C_Q \cos\Theta(1+\cos\Theta)$ and an example is shown in the Supporting Information. The value of $\bar{C}_Q$ for any other orientational distribution has to be evaluated numerically. For the grafted molecule, the time dependence of the $\bar{d}_3$ vector can be mapped on a unit sphere at equal time intervals, as is shown in the Supporting Information, Figure S3. The aim of the MD simulation is thus to monitor the orientation of the $\bar{d}_3$ vector as a function of time, to represent its direction on a unit sphere and to calculate the average values $\{\bar{C}_Q, \bar{\eta}\}$.

i. Dehydrated Surface with No Nearby Hydroxyl Groups. To create the covalent attachment of the molecule through two oxygen atoms to the surface, initially the molecule in its T_2 configuration was drawn in the MS visualizer and subjected to a DISCOVER minimization. This resulted in an "all-trans" minimized conformation of the chain of the molecule, as expected for a linear molecule. The stabilized T_2 configuration was then covalently attached to the surface through two oxygen atoms by breaking a Si−O−Si linkage of the dehydrated stabilized mesoporous surface. The system as a whole was again subjected to a DISCOVER minimization process. The overall minimization took less than 1 h in a server utilizing four processors.

FORCITE dynamic simulations were performed starting from this minimized system using the COMPASS force field. The system was initially equilibrated through a dynamic calculation for 700 ps. All further calculations were performed by keeping the equilibrated structure as the starting

dx.doi.org/10.1021/jp3061152 | J. Phys. Chem. B 2012, 116, 10398−10405

conformation. Two picosecond dynamic simulations with a time step of 1 fs for the integration of the equations of motion were carried out for two different temperatures 330 and 280 K. Each 1000th molecular conformation was saved as a trajectory file. At the end, the coordinates of all atoms of the molecule, including the molecular segment C(O)−C(D_3) defining $\overline{d}_3$, were extracted using a Perl program and exported to MATLAB for further analysis. These coordinates were defined in a reference frame determined by the coordinate system defined by the MD program during the calculation. To represent the time dependence of $\overline{d}_3$, we chose a coordinate system with its *z*-axis perpendicular to the surface and the *x*-axis pointing in the direction of the vector connecting the oxygen atoms binding the molecule to the surface. The coordinates of the atoms extracted from the MD simulations were transformed to this new frame.

Initial dynamic simulations were performed, for a temperature set at 330 K, for a grafted molecule bound to the surface after removing all hydroxyl groups in the vicinity of the binding site. As a result, the $\overline{d}_3$ vector occupied three distinct regions on the unit sphere of $\{\theta, \varphi\}$ angles. However, the trans-conformation is occupied more than 70% of the time, indicating that this is the major conformation of the grafted molecules. This is shown in Figure 6a where the $\overline{d}_3$ dots on the unit sphere are mainly located around $\{\theta \sim 120°; \varphi \sim 80°\}$. The corresponding $\{\overline{C}_Q; \overline{\eta}\}$ values can therefore not deviate significantly from the original $\{\overline{C}_Q \sim 75$ kHz; $\overline{\eta} = 0\}$ values. Comparing this result with the experiments indicates that this situation can explain only the static CD_3 spectral components.

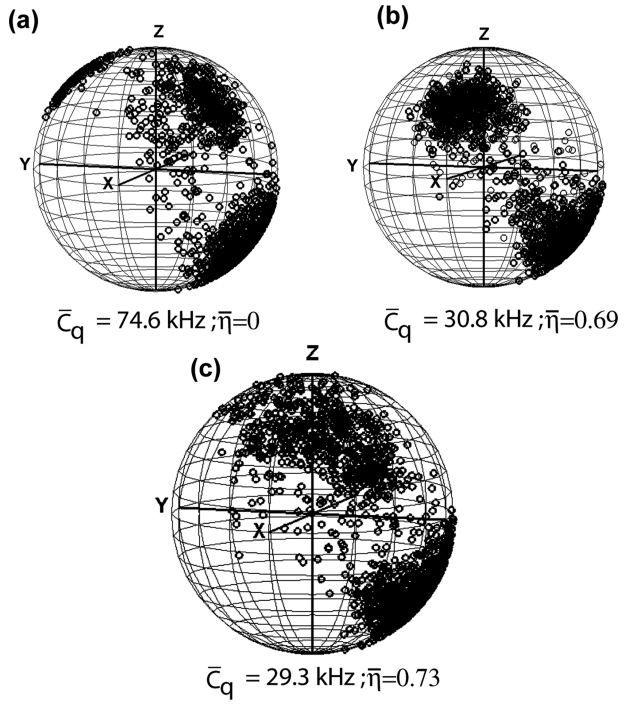

Figure 6. Distribution of the trajectory vectors derived from MD representing the spatial variation of CO−CD_3 drawn on a unit sphere. The molecule was anchored in the T_2 conformation on a dehydrated surface with (a) no hydroxyls nearby, (b) a hydroxyl group adjacent to one of the anchored oxygen atoms by 2.63 Å, and (c) a hydroxyl group adjacent to the anchored oxygen atom by 4.613 Å. The respective average quadrupolar parameters are shown below the sphere. In all the three cases MD calculation was performed at 330 K.

ii. Dehydrated Surface with Nearby Hydroxyl Groups. As an attempt to monitor mobility induced by hydroxyl groups, we have rehydrated the silica surface around the binding site. As a first trial, the surface oxygen next to one of the binding oxygen atoms was hydrated with two hydroxyl groups. The distance between one of the oxygens to which the molecule is bound to the adjacent oxygen of the hydroxyl is 2.63 Å. With a hydroxyl surface density of about 2.2 per nm^2, and realizing that the length of the chain at its "all-trans" conformation is about 7.68 Å, it is reasonable to assume that in practice the probability of additional −OH groups in the neighborhood of the molecule is rather small. The result of the subsequent MD calculation for this system is shown in Figure 6b. From the vector distribution, the average quadrupolar parameters obtained are $\{\overline{C}_Q = 30.8$ kHz; $\overline{\eta} = 0.69\}$. This is well in agreement with the experimental observation presented above. Inspection of the $\overline{d}_3$ vector distribution suggests that there are two main conformations resulting in two areas on the sphere, indicative of a two-site jump motion of the CD_3 group.

The result of a second example attempting to simulate the molecular motion of the grafted molecule is shown in Figure 6c. For this simulation an oxygen atom that was situated 4.613 Å away from one of the binding oxygens was hydrated. Here again a two-site exchange dynamics is clearly observed resulting in the values $\{C_Q = 29.5\ kHz; \overline{\eta} = 0.72\}$. Both (b) and (c) provided similar average quadrupole parameters, indicating that different two-site jump motions can explain the experimental observations.

iii. Molecular Conformations Associated with the Two-Site Exchange. To study the reorientational motion resulting in the two-site exchange of the CD_3 groups in the first example (Figure 6b), we show in Figure 7 the time dependence of the angle θ of the $\overline{d}_3$ vector as well as the dihedral angles defining the structure of the chain. A careful observation shows that there are three main conformations, one (A_1) corresponding to the almost "all−trans" conformation with a set of polar angles

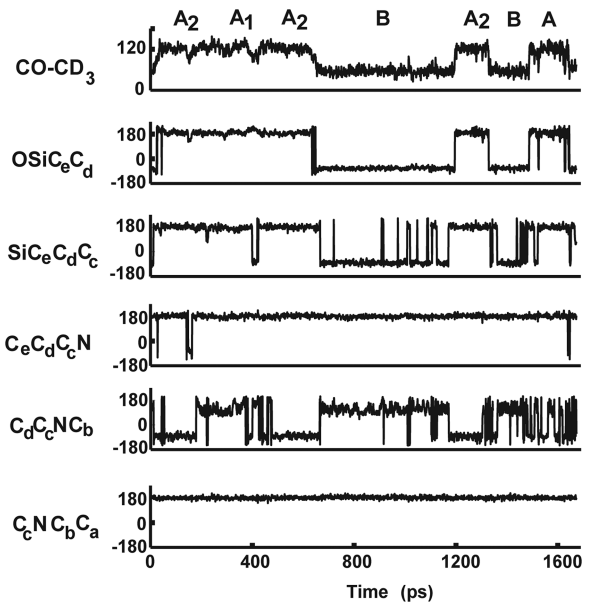

Figure 7. Time dependence of various angles of the molecule along its chain. The conditions for MD correspond to those of Figure 6b. A($_{1,2}$) and B represent the two conformers representing the two-site jump motion.

dx.doi.org/10.1021/jp3061152 | *J. Phys. Chem. B* 2012, 116, 10398−10405

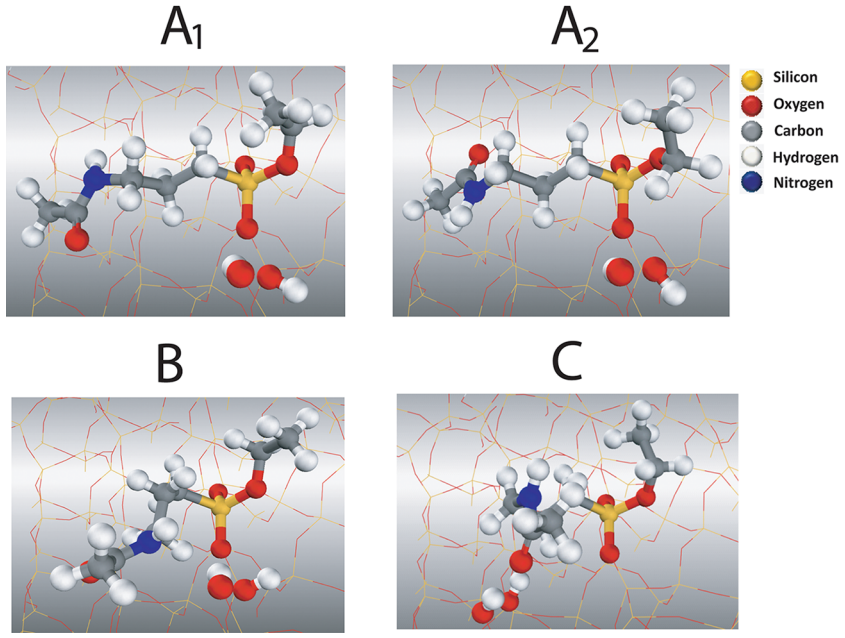

Figure 8. Molecular conformation as obtained from the MD. $A_{(1,2)}$ represents the initial equilibrium conformation of the molecule bound to the surface. When the molecule undergoes dynamics, the conformation changes from $A_{(1,2)}$ to B or C, resulting in average quadrupolar parameters.

$\{\theta, \varphi\}$ equal to $\{121 \pm 30, 74 \pm 30\}$ and a second conformation (A_2) with about the same polar angles. For the third conformation (B) the distance between the amide proton and the oxygen of one of the hydroxyl groups, −NH---OH−, varies between 2.417 and 1.83 Å, indicative of a possible hydrogen bonding stabilization of this conformation. Reconstructions of the average conformations of ($A_{1,2}$) and (B) are shown in Figure 8. Results of simulations carried out at 280 K are also shown (Supporting Information, Figure S4). In this case the average jump rate between the conformations is slower than at 330 K.

For the second example the conformational changes, in terms of dihedral angles, of the chain of the grafted molecule are shown in the Supporting Information (Figure S5). Here again we can distinguish three major conformations, two of them close to the "all-trans" conformation an one a bend conformation. The second one shows a −NH---OH− distance of more than 4.6 Å and a shortest carbonyl to hydroxyl, −CO---OH−, distance between 2.53 and 1.86 Å.

iv. Dehydrated Surface with Removed Hydroxyl Groups. Positioning the hydroxyl groups at additional positions, not equivalent to the first two examples did not result in new binding conformations that lower the average coupling constant. In the Supporting Information, Figure S6, an example of the chain motion with a hydroxyl groups positioned from the molecule by 6.3 Å is presented. As shown in the Supporting Information (Figure S7), the results resemble the motion without any hydroxyl group in neighborhood. The existence of a two-site exchange process can thus only be expected when the hydroxyl groups reside closer than about 5 Å from one of the anchoring oxygens.

CONCLUSION

In the present work we have interpreted the experimental data from observations derived from MD simulations. No a priori assumption of a dynamic model for the $\bar{d}_3$ motion was made. MD simulations were performed on a grafted molecule bound to a low hydrated surface, where on average we expect none or one hydroxyl pair in its neighborhood. The analysis of the time dependent polar angles of $\bar{d}_3$, resulting from the MD simulations on molecules without or one hydroxyl pair nearby, provided values for the average quadrupole parameters of its CD_3 group that are about equal to the experimental values of the static and dynamic spectra. The static spectrum corresponds to the almost "all-trans" configuration and the dynamic spectra to exchanging molecules between an "all-trans" and a bend configuration. The bend structures seemed to be stabilized by −NH---OH− or −CO---OH− bindings. By exploiting MD simulations, it has been possible to suggest a dynamic model for the grafted molecules.

Single water molecules seem to play an important role in supporting the two-site exchange mobility of the grafted molecules. The deuterium MAS data have shown that the fraction of dynamic molecules increases for increasing temperature and increasing water content. Together with this increase the average quadrupole parameters change as well. From the change in the relative amounts of the dynamic molecules we can conclude that the addition of two hydroxyl groups per nm^2 is sufficient at 315 K to increase the ratio between dynamic and static molecules by a factor of 2. Presumably, the water protons perform a slow exchange with the hydroxyl protons of the surface increasing possibly the number of hydroxyls accessible for hydrogen bonding with the amide or carbonyl groups.

The combination of ^2H MAS NMR and MD simulations for the characterization of the motion of single grafted molecules could be easily extended to additional similar systems or bound molecular monolayers. This is in particular relevant for fast motional processes where MD simulations in time periods of up to a few nanoseconds range can be utilized to support the interpretation of ^2H MAS spectra exhibiting narrow sideband patterns.

dx.doi.org/10.1021/jp3061152 | J. Phys. Chem. B 2012, 116, 10398−10405

■ ASSOCIATED CONTENT

Supporting Information

Additional information about the characterization of the grafted system using solid state NMR; numerical model used to interpret the MD output; MD simulations performed at different conditions. This material is available free of charge via the Internet at http://pubs.acs.org.

■ AUTHOR INFORMATION

Corresponding Author

*E-mail: Shimon.Vega@weizmann.ac.il.

Notes

The authors declare no competing financial interest.

■ ACKNOWLEDGMENTS

We thank Prof. A. Schmidt and his group for fruitful discussions and also for providing experimental time on the AVIII- 500 & 300 MHz spectrometers. This research was supported by the Grant from GIF, the German−Israeli Foundation for Scientific Research and Development (Grant No. 76/2009). S.J. thanks Dr. Vikrant Vijay Naik (*Surface Science and Technology, ETH-Zurich*) for many stimulating discussions related to Molecular Dynamic simulations. This research is made possible in part by the historic generosity of the Harold Perlman family.

■ REFERENCES

(1) Jing, H.; Xiaofen, L.; Evans, D. J.; Xue, D.; Chengyue, L. *J. Mol. Catal.* **2000**, *11*, 45−53.

(2) Takahashi, H.; Li, B.; Sasaki, T.; Miyazaki, C.; Kajino, T.; Inagaki, S. *Microporous Mesoporous Mater.* **2001**, *44*−*45*, 755−762.

(3) Pages, G.; Delaurent, C.; Caldarelli, S. *Anal. Chem.* **2006**, *78*, 561−566.

(4) Yurong, M. L. Q.; Jiming, M.; Yongqing, W. O. L.; Humming, C. *Colloids Surf., A* **2003**, *229*, 1−8.

(5) Wang, Q.; Jordan, E.; Shantz, D. F. *J. Phys. Chem C* **2009**, *113*, 18142−18151.

(6) Zhang, W.; Ratcliffe, C. I.; Moudrakovski, I. L.; Tse, J. S.; Mou, C.-Y.; Ripmeester, J. H. *Microporous Mesoporous Mater* **2005**, *79*, 195−203.

(7) Qiao, S. Z.; Bhatia, S. K. *Ind. Eng. Chem. Res.* **2005**, *44*, 6477−6484.

(8) Masierak, W.; Emmler, Th.; Schreiber, E.; Findenegg, G. H.; Buntkowsky, G. *Phys. Chem. Chem.. Phys.* **2004**, *108*, 18890−18896.

(9) Grünberg, B.; Emmler, T.; Gedat, E.; Shenderovich, I.; Findenegg, G. H.; Limbach, H. H.; Buntkowsky, G. *Chem. Eur, J.* **2004**, *10*, 5689−5696.

(10) Vyalikh, A.; Emmler, Th.; Shenderovich, Y. Z.; Findenegg, G. H.; Buntkowsky, G. *Phys. Chem. Chem.. Phys.* **2007**, *9*, 2249−2257.

(11) Kintzel, E. J., Jr.; Kidder, M. K.; Buchanan, A. C.; Britt, P. F.; Mamonotov, E.; Zamponi, M.; Herwig, K. W. *J. Phys. Chem. C* **2012**, *116*, 923−932.

(12) Pizzanelli, S.; Kababya, S.; Frydman, V.; Landau, M.; Vega, S. *J. Phys. Chem. B* **2005**, *109*, 8029−8039.

(13) A-Rosen, T.; Kababya, S.; Vega, S. *J. Phys. Chem. B* **2009**, *113*, 6267−6282.

(14) A-Rosen, T.; Vega, S. *Phys. Chem. Chem. Phys* **2010**, *12*, 6763−6773.

(15) Waechtler, M.; Selin, M.; Stark, A.; Akcakayiran, D.; Buntkowsky, G. *Phys. Chem. Chem. Phys.* **2010**, *12*, 11371−11379.

(16) Ladizhansky, V.; Hodes, G.; Vega, S. *J. Phys. Chem. B* **2000**, *104*, 1939−1943.

(17) Gedat, E.; Schreiber, A.; Albrecht, J.; Emmler, Th.; Findenegg, G. H.; Limbach, H. H.; Buntkowsky, G. *J. Phys. Chem. B.* **2002**, *106*, 1977−1984.

(18) Ben Shir, I.; Kababya, S.; A-Rosen, T.; Balazs, Y. S.; Schmidt, A. *J. Phys. Chem. B* **2010**, *114*, 5989−5996.

(19) Ben. Shir, I.; Kababya, S.; Schmidt, A. *J. Phys. Chem. C* **2012**, *116*, 9691−9702.

(20) Schaefer, J.; Sefcik, M. D.; Stejskal, E. O.; McKay, R. A.; Dixon, W. T. *Macromolecules* **1984**, *17*, 1107−1118.

(21) Schaefer, J.; Stejskal, E. O.; McKay, R. A. *J. Magn. Reson.* **1984**, *57*, 85−92.

(22) Hentschel, D.; Sillescu, H.; Spiess, H. W. *Makromol. Chem.* **1979**, *180*, 241−267.

(23) Spiess, H. W.; Silescu, H. *J. Magn. Reson.* **1979**, *35*, 157−162.

(24) Hentschel, D.; Sillescu, H.; Spiess, H. W. *Macromolecules* **1981**, *14*, 1605−1712.

(25) Collignon, J.; Sillescu, H.; Spiess, H. W. *Colloid Polym. Sci.* **1981**, *259*, 220−226.

(26) Spiess, H. W. *Adv. Polym. Sci.* **1985**, *66*, 23−58.

(27) Jelinski, L. W.; Dumais, J. J.; Engel, A. K. *Macromolecules* **1983**, *16*, 492−96.

(28) Jelinski, L. W.; Dumais, J. J.; Cholli, A. L. *Polym. Prepr. Am. Chem. Soc. Div. Polym. Chem.* **1984**, *25*, 348−350.

(29) Cholli, A. L.; Dumais, J. J.; Engel, A. K.; Jelinski, L. W. *Macromolecules* **1984**, *17*, 2399−2404.

(30) Buchanan, G. W.; McManus, G.; Jarrel, H. C. *Chem. Phys. Lipids* **2003**, *104*, 23−34.

(31) Alam, T. M.; Orban, J.; Drobny, G. P. *Biochemistry* **1991**, *30*, 9229−9237.

(32) Alam, T.; Drobny, G. P. *Chem. Rev.* **1991**, *91*, 1545−1590.

(33) de Gennes, P. G. *J. Chem. Phys.* **1971**, *55*, 572−580.

(34) Naik, V. N.; Vasudevan, S. *J. Phys. Chem. C* **2009**, *113*, 8806−8813.

(35) Torchia, D. A.; Szabo, A. *J. Magn. Reson.* **1982**, *49*, 107−121.

(36) Nawrocki, J. *J. Chromatogr., A* **1997**, *779*, 29−71.

(37) Zhuravlev, L. T. *Colloids Surf., A* **1997**, *779*, 29−71.

(38) Pines, A.; Gibby, M. G.; Waugh, J. S. *J. Chem. Phys.* **1973**, *53*, 569−590.

(39) Bak, M.; Rasmussen, J. T.; Nielsen, N. Chr. *J. Magn. Reson.* **2000**, *147*, 296−330.

(40) *Materials Studio*, Version 5.5; Accerelys Software, Inc.: San Diego, CA, 2010.

(41) Maple, J. R.; Hwang, M. J.; Stockfisch, T. P.; Dinur, U.; Waldman, M.; Ewig, C. S.; Hagler, A. T. *J. Comput. Chem.* **1994a**, *15*, 162−182.

(42) Sun, H. *J. Phys. Chem. B* **1998**, *102*, 7338−7384.

(43) Sun, H. *Macromolecules* **1995**, *28*, 701.

(44) Chaffe, A. L. *Fuel Proc. Tech.* **2005**, *86*, 1473−1486.